ChemComm

Self-assembled reversed bilayers directed by pnictogen bonding to form vesicles in solution.

Journal:	*ChemComm*
Manuscript ID	CC-COM-06-2018-005187.R1
Article Type:	Communication

ChemComm

COMMUNICATION

Self-assembled reversed bilayers directed by pnictogen bonding to form vesicles in solution.

Received 00th January 20xx,
Accepted 00th January 20xx

DOI: 10.1039/x0xx00000x

www.rsc.org/

Shiva Moaven, Jingze Yu, Maythe Vega, Daniel K. Unruh, Anthony F. Cozzolino*

Artificial vesicles can aid in the study and understanding of biological cell membranes. This study employs pnictogen bonding to actively direct the self-assembly of a true reversed bilayer. Antimony(III) alkoxide cages that self-assemble through multiple strong Sb···O interactions propagate in two dimensions to form a reverse bilayer structure in the solid state. Long alkyl tails allow these reverse bilayers to be processed into vesicles in solution that are a reverse of biological cell membranes.

Vesicles play a crucial role in biological systems. Extracellular vesicles, for example, are the main transportation system used to carry proteins, genes, and chemicals.[1,2] To understand the biophysical processes of the natural cell membranes, artificial vesicles have been self-assembled from both natural or artificial building blocks (Figure 1, normal bilayer) and their physical and chemical behaviors have been explored during the last few decades.[1,3–5] Inverting the normal bilayers result in the formation of lipophilic membranes which can have unique properties including solubility in non-polar solvents.[6,7] The first such membranes, described by Kunieda et al, used small amounts of water to stabilize the hydrophilic heads of tetraethylene glycol dodecylether in a nonpolar solvent (Figure 1, reversed trilayer). They named these supramolecular structures "reversed vesicles".[6,8–11] Other examples of lipophilic membranes were reported later using similar methods to self-assemble ionic or zwitterionic surfactants using solvent mixtures or salts to stabilize the hydrophilic heads.[7,12–14] Examples that do not require a second component to organize the heads have also been reported. In these cases the tails are either preassembled through coordination to a metal or metal cluster,[15–18] or by covalent attachment to a core.[19,20] Self-assembly of these units into monolayers occurs

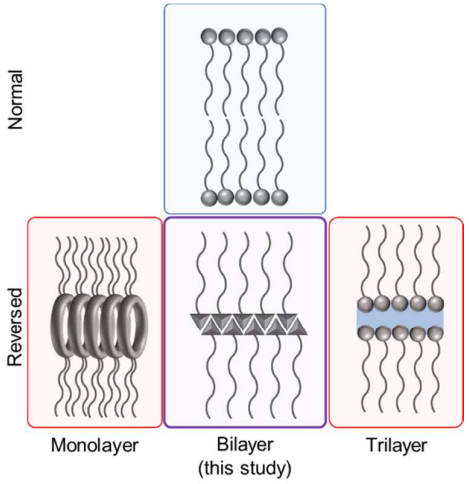

Fig. 1 Schematic representation of natural hydrophilic bilayers (top) and different arrangements to produce reversed lipophilic membranes (bottom).

(Figure 1, reversed monolayer) and can be facilitated by hydrogen bonding.[19]

While the aforementioned examples of lipophilic membranes represent exciting strategies for achieving a functional inversion of the biological bilayer, they do not represent strategies that are direct analogues of nature. To achieve this, we propose to utilize supramolecular interactions that can propagate self-assembly in two dimensions; in particular, the secondary bonding interactions (SBIs) of the heavy pnictogens, or *pnictogen bonding*.

The ability of the heavy p-block elements to form additional weak interactions beyond their primary valency was recognized as a general phenomenon as early as 1968.[21–23] In the past two decades, many exciting advances have been made by utilizing iodine-centered interactions, termed *halogen bonding*.[24] The chalcogens and pnictogens have seen less progress, despite their ability to form stronger interactions.[25–29] Halogen bonds are topologically analogous to hydrogen bonds, so similar motifs can be employed when designing systems that self-

Department of Chemistry and Biochemistry, Texas Tech University, Box 41061, Lubbock, Texas 79409-1061, United States. E-mail: anthony.f.cozzolino@ttu.edu.
Electronic Supplementary Information (ESI) available: synthesis and preparation of the materials and vesicles, ^{1}H NMR, ^{13}C NMR, ATR-FTIR, DLS, TEM and SEM. **2** (CCDC 1843709)]. See DOI: 10.1039/x0xx00000x

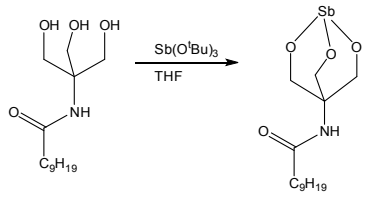

Scheme 1 Synthesis of 2.

assemble through halogen bonding. Chalcogen and pnictogen bonding requires a more de novo approach as they can accommodate two or three distinct interactions per element. Here, much inspiration can be derived from motifs found in crystal structures.[28,30]

Recently we reported on antimony alkoxide cages that self-assemble through multiple Sb···O pnictogen bonds.[28] The self-assembly was found to be predictable owing to the strength and directionality of these interactions. It was determined that the length of the appended alkyl chain could be used to direct the self-assembly process to form bilayers in the solid state. The current study expands on this concept through the design of systems that self-assemble into a bilayer in the solid state but can be processed in solution to generate vesicles that are self-assembled through pnictogen bonds. Here, these predictable interactions control the formation of bilayers that are reversed from the typical lipid bilayers and suggest a new approach to attaining such features in solution.

In order to attain a solution-processable antimony(III) alkoxide cage, a long aliphatic tail was installed on the cage. Tris(hydroxymethyl)aminomethane was acylated with decanoyl chloride to produce *N*-[2-hydroxy-1,1-bis(hydroxymethyl)ethyl]-decanamide (**1**).[31,32] Treatment of a THF solution of **1** with antimony(III) *tert*-butoxide resulted in the formation of the antimony(III) alkoxide cage compound **2** (Scheme 1) which could be isolated cleanly by filtration (see SI for details). As has been noted for other systems with multiple strong chalcogen or pnictogen bonds, solvents with large E_B Drago-Wayland parameters, such as pyridine, DMSO or DMF, are needed to compete with the intermolecular interactions to allow for complete dissolution.[28,33] Compound **2** only dissolves in these solvents upon heating. This corroborates the high electrostatic contribution to these pnictogen bonds.

Formation of **2** was confirmed through ^{1}H NMR (see Figure S3) in d_6-DMSO by the absence of the hydroxyl proton triplet at 4.77 ppm and marked shifts (0.72 ppm) of the cage methylene protons. A similar shift of 8.45 ppm for the methylene carbons was observed in the ^{13}C NMR spectrum. Both of these shifts are consistent with those previously reported for antimony alkoxide cage formation.[28] FTIR spectroscopy also confirmed the disappearance of the hydroxyl group O–H stretch at 3286 cm^{-1} (Figure S7). The formation of SBIs was probed by evaluating the energy of the Sb–O stretches of **2** and contrasting them with the energy of antimony alkoxides that do not self-assemble. The FTIR of **2** reveals a stretching frequency for **2** (492 cm^{-1}, Figure S7) that is well shifted from the Sb–O stretching frequency of monomeric antimony(III) *tert*-butoxide (587 cm^{-1}).[28] This is

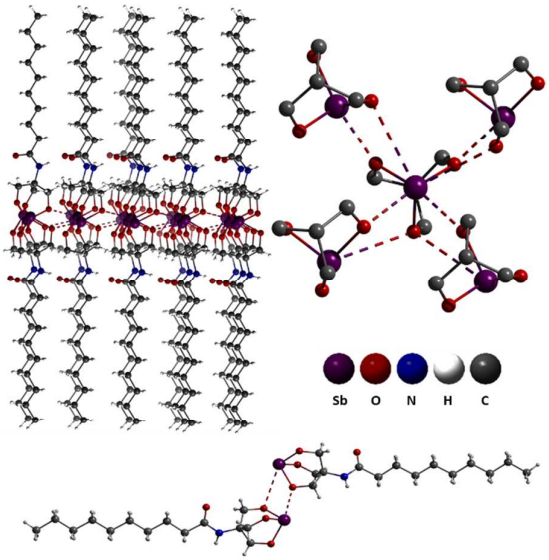

Fig. 2 Top left: ball and stick representation of reversed bilayers from self-assembly of 2 in solid state crystal structure. Top right: self-assembly pattern around central molecule of 2 (hydrogens and tails are omitted for clarity). Bottom: representation of a dimeric unit in crystal structure of 2.

consistent with the weaker Sb–O bonds that exist in the self-assembled structures.[28,34,35] This is consistent with the conceptual model where the secondary bond formation results, in part, from donation of electron density into the Sb–O σ* orbital.[23]

X-ray quality single crystals of **2** (Fig. **2**, CCDC 1843709) were grown from a saturated solution of **2** in DMSO. Similar to the previously reported antimony alkoxide cage that forms a bilayer in the solid state, each molecule of **2** interacts with four additional antimony cages through pnictogen bonds in an antiparallel arrangement. This connectivity results in the inverted 2D bilayer structure as depicted in Figure 1. It is notable that the shortest amide-amide N···O distance is 3.466(6) Å. This is well above typical distances associated with strong amide-amide hydrogen bonds.[36] This suggests that, not only do pnictogen bonds direct the bilayer formation, but that they do so in the presence of groups that can competitively hydrogen bond to give a motif that is consistent with the one previously observed in the solid state without groups that could form strong hydrogen bonds. [28] The aliphatic chains in neighboring bilayers interdigitate to complete the third dimension of the lattice. The PXRD of the bulk sample isolated from THF was consistent with the simulated powder X-ray diffraction pattern of the single crystal data.

The goal of the elongated structure was to make the system amenable to solution studies. Dry acetone was determined to be an ideal solvent for manipulating **2**. It is notable that acetone has a Drago-Wayland E_B parameter in between pyridine (**2** is soluble) and THF (**2** is insoluble). Dynamic light scattering (DLS) was used to determine the size distribution of particles of **2**. Solutions with concentrations ranging from 0.05–0.5 μM of **2** in dry acetone were prepared and sonicated

for 10 seconds, 2 minutes, or 5 minutes (Figures S8-S12). Regardless of the sonication time, concentrations above 0.3 μM resulted in the formation of particles with broad size distributions ranging from 0.1–4 μm. These solutions were visibly opaque (Figure S9). Lower concentrations with longer sonication times resulted in the formation of homogeneous solutions (Figure S13). These solutions contained particles with a narrower size distribution, ranging from 40–200 nm (Fig. **3**). The ^{1}H NMR of these homogeneous solutions did not reveal any signals. This would

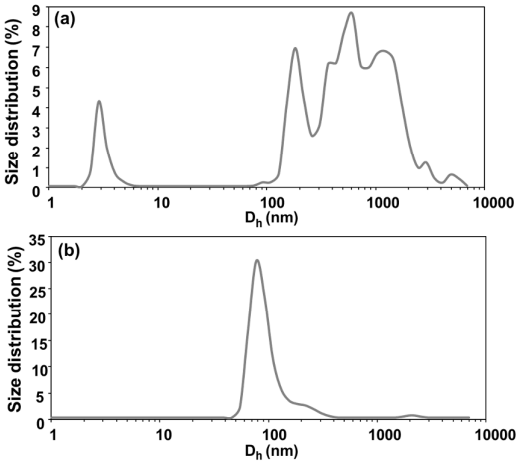

Fig. 3 DLS particle size distributions of (a) 0.5 μM and (b) 0.05 μM solutions of 2 in acetone after sonication for 5 minutes.

be consistent with the molecules being in a non-fluctional environment. This contrasts with observable signals in DMSO-d_6 which can readily form strong SBIs with antimony(III) which keep it dissociated in solution.[37,38]

TEM was used to determine the nature of the particles produced under different conditions and to specifically probe for evidence of hollow vesicles. Samples were prepared under an inert atmosphere in dry acetone and cast on a copper grid coated with carbon. The excess solvent was absorbed by filter paper placed under the grid. Samples with short sonication times or high concentrations yielded images containing large, opaque particles consistent with the heterogeneous appearance of the solution (Figure S9 and S15).

Samples of **2** in acetone ranging in concentration from 0.05 to 0.15 μM, which appeared homogeneous to the eye, yielded TEM images such as those shown in Figure S13. Here, no evidence of the opaque solid particles was observed. Rather, the particles were on the nanometer scale and appear to have circular shapes with a hollow interior (Fig. **4**). The dark rings, which represent regions of low transparency, are consistent with regions of high electron density. This is consistent with a model in which the bilayer structure seen in the crystal structure, which concentrates the electron-rich antimony atoms together, is retained to create self-assembled inverted bilayer vesicles in solution directed by Sb···O SBIs.

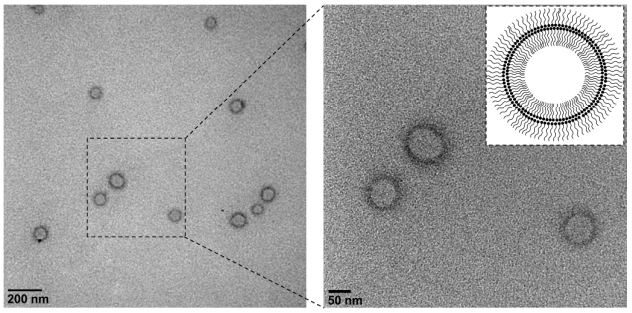

Fig. 4 TEM images at two magnifications of 2 after sonication of a 0.075 μM dry acetone solution for 5 minutes. Inset contains a sketch of a cross-section of a reversed bilayer vesicle consistent with self-assembly in the solid-state structure.

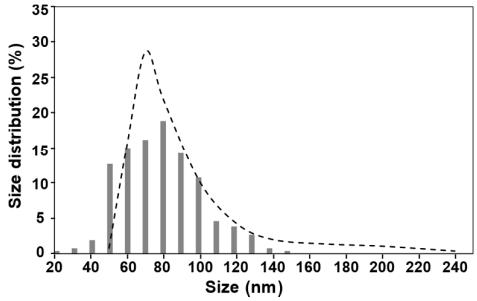

Fig. 5 Histograms: size distribution of vesicles. Measurements were made from 150 vesicles in two TEM images (See figure S14). Dotted line: overlay of DLS results of 0.05 μM concentration after 5 minutes sonication.

Fig. **5** shows a comparison of the distribution of particle sizes in the TEM images (see Figure S14) as compared with the distribution from the DLS measurements. Most of the measured vesicle diameters from the TEM images range from 50–100 nm and are consistent with the DLS measurements.

SEM images were obtained from samples prepared using the same method that was used for the TEM images. The vesicles were sensitive to the electron beam and during image capturing would change size and vibrate. This made imaging single vesicles difficult. Fig. **6** shows an agglomerate of vesicles of **2**. Notably, in the well-dispersed sample, few of these agglomerates exist. Corrections were applied to highlight the spherical morphology of these vesicles (the original image and a description of the corrections are provided in Figure S16). The individual vesicles in the agglomerate are consistent with the sizes measured by DLS and TEM. Agglomeration of these vesicles likely results from the interdigitation of the exposed exterior alkyl chains in a manner similar to what is observed in the crystal structure.

In summary, a synthetic method to produce amphiphilic antimony(III) alkoxides that will self-assemble in two dimensions to form an inverted bilayer in both the solid and solution states is reported. Hollow vesicles of **2** were prepared in acetone using ultrasonication. These vesicles are expected to have self-assembled through the homo-molecular pnictogen bonding (Sb···O) of molecules of **2** in a manner consistent with the solid-state structure. This results in the formation of reversed bilayer vesicles that are the first true inverted analogue of biological self-assembled bilayer membranes.

Fig. 6 SEM image vesicles of 2 (0.075μM solution sonicated for 5 minutes).

A.F.C. and S.M. are grateful for financial support from the Robert A. Welch Foundation (D-1838, USA), Texas Tech University and the National Science Foundation (NMR instrument grant CHE-1048553). J.Y. and M.V. are grateful for financial support from the Welch Summer Scholar Program. Dr. Hope-Weeks is thanked for access to DLS.

Notes and references

1 F. Fernandez-Trillo, L. M. Grover, A. Stephenson-Brown, P. Harrison and P. M. Mendes, *Angew. Chem. Int. Ed.*, 2017, **56**, 3142–3160.
2 T. Lener, M. Gimona, L. Aigner, V. Börger, E. Buzas, G. Camussi, N. Chaput, D. Chatterjee, F. A. Court, H. A. del Portillo, L. O'Driscoll, S. Fais, J. M. Falcon-Perez, U. Felderhoff-Mueser, L. Fraile, Y. S. Gho, A. Görgens, R. C. Gupta, A. Hendrix, D. M. Hermann, A. F. Hill, F. Hochberg, P. A. Horn, D. de Kleijn, L. Kordelas, B. W. Kramer, E.-M. Krämer-Albers, S. Laner-Plamberger, S. Laitinen, T. Leonardi, M. J. Lorenowicz, S. K. Lim, J. Lötvall, C. A. Maguire, A. Marcilla, I. Nazarenko, T. Ochiya, T. Patel, S. Pedersen, G. Pocsfalvi, S. Pluchino, P. Quesenberry, I. G. Reischl, F. J. Rivera, R. Sanzenbacher, K. Schallmoser, I. Slaper-Cortenbach, D. Strunk, T. Tonn, P. Vader, B. W. M. van Balkom, M. Wauben, S. E. Andaloussi, C. Théry, E. Rohde and B. Giebel, *J. Extracell. Vesicles*, 2015, **4**, 30087.
3 S. Matosevic and B. M. Paegel, *Nat. Chem.*, 2013, **5**, 958–963.
4 G. Stengel, R. Zahn and F. Höök, *J. Am. Chem. Soc.*, 2007, **129**, 9584–9585.
5 J. Voskuhl and B. Jan Ravoo, *Chem. Soc. Rev.*, 2009, **38**, 495–505.
6 H. Kunieda, K. Nakamura and D. F. Evans, *J. Am. Chem. Soc.*, 1991, **113**, 1051–1052.
7 S.-H. Tung, H.-Y. Lee and S. R. Raghavan, *J. Am. Chem. Soc.*, 2008, **130**, 8813–8817.
8 H. Kunieda, M. Akimaru, N. Ushio and K. Nakamura, *J. Colloid Interface Sci.*, 1993, **156**, 446–453.
9 H. Kunieda, K. Nakamura, U. Olsson and B. Lindman, *J. Phys. Chem.*, 1993, **97**, 9525–9531.
10 U. Olsson, K. Nakamura, H. Kunieda and R. Strey, *Langmuir*, 1996, **12**, 3045–3054.
11 H. Kunieda, K. Shigeta and M. Suzuki, *Langmuir*, 1999, **15**, 3118–3122.
12 H. Li, J. Hao and Z. Wu, *J. Phys. Chem. B*, 2008, **112**, 3705–3710.
13 H. Li, X. Xin, T. Kalwarczyk, E. Kalwarczyk, P. Niton, R. Hołyst and J. Hao, *Langmuir*, 2010, **26**, 15210–15218.
14 H. Li, X. Xin, T. Kalwarczyk, R. Hołyst, J. Chen and J. Hao, *Colloids Surf. Physicochem. Eng. Asp.*, 2013, **436**, 49–56.
15 H. Li, H. Sun, W. Qi, M. Xu and L. Wu, *Angew. Chem. Int. Ed.*, 2007, **46**, 1300–1303.
16 W. Li, B. Li, Y. Wang, J. Zhang, S. Wang and L. Wu, *Chem. Commun.*, 2010, **46**, 6548–6550.
17 R. Dong and J. Hao, *ChemPhysChem*, 2012, **13**, 3794–3797.
18 H.-Y. Lee, K. Hashizaki, K. Diehn and S. R. Raghavan, *Soft Matter*, 2012, **9**, 200–207.
19 X.-N. Xu, L. Wang and Z.-T. Li, *Chem. Commun.*, 2009, **0**, 6634–6636.
20 K.-D. Zhang, T.-Y. Zhou, X. Zhao, X.-K. Jiang and Z.-T. Li, *Langmuir*, 2012, **28**, 14839–14844.
21 H. A. Bent, *Chem. Rev.*, 1968, **68**, 587–648.
22 O. Hassel, *Science*, 1970, **170**, 497–502.
23 N. W. Alcock, in *Advances in Inorganic Chemistry and Radiochemistry*, ed. H.J. Emeléus and A.G. Sharpe, Academic Press, 1972, vol. Volume 15, pp. 1–58.
24 P. Metrangolo and G. Resnati, *Chem. - Eur. J.*, 2001, **7**, 2511–9.
25 L. Brammer, *Faraday Discuss.*, 2017, **203**, 485–507.
26 S. Benz, J. Mareda, C. Besnard, N. Sakai and S. Matile, *Chem. Sci.*, 2017, **8**, 8164–8169.
27 A. F. Cozzolino, P. J. W. Elder, L. M. Lee and I. Vargas-Baca, *Can. J. Chem.*, 2013, **91**, 338–347.
28 S. Moaven, J. Yu, J. Yasin, D. K. Unruh and A. F. Cozzolino, *Inorg. Chem.*, 2017, **56**, 8372–8380.
29 G. E. Garrett, E. I. Carrera, D. S. Seferos and M. S. Taylor, *Chem. Commun.*, 2016, **52**, 9881–9884.
30 V. M. Cangelosi, M. A. Pitt, W. J. Vickaryous, C. A. Allen, L. N. Zakharov and D. W. Johnson, *Cryst. Growth Des.*, 2010, **10**, 3531–3536.
31 A. Unciti-Broceta, L. Moggio, K. Dhaliwal, L. Pidgeon, K. Finlayson, C. Haslett and M. Bradley, *J. Mater. Chem.*, 2011, **21**, 2154–2158.
32 E. Bieberich, B. Hu, J. Silva, S. MacKinnon, R. K. Yu, H. Fillmore, W. C. Broaddus and R. M. Ottenbrite, *Cancer Lett.*, 2002, **181**, 55–64.
33 A. F. Cozzolino, J. F. Britten and I. Vargas-Baca, *Cryst. Growth Des.*, 2006, **6**, 181–186.
34 B. A. Arbuzov, R. R. Shagidullin, V. S. Vinogradova, I. K. Shakirov and Y. M. Mareev, *Bull. Acad. Sci. USSR Div. Chem. Sci.*, 1980, **29**, 1270–1275.
35 B. A. Arbuzov, Y. M. Mareev, R. R. Shagidullin, V. S. Vinogradova and I. K. Shakirov, *Bull. Acad. Sci. USSR Div. Chem. Sci.*, 1984, **33**, 1686–1691.
36 G. Desiraju and T. Steiner, *The Weak Hydrogen Bond*, Oxford University Press, Oxford, 1999.
37 J. M. Tanski, B. V. Kelly and G. Parkin, *Dalton Trans.*, 2005, 2442–2447.
38 D. Mendoza-Espinosa and T. A. Hanna, *Inorg. Chem.*, 2009, **48**, 10312–10325.

Vesicles with a reversed bilayer membrane are self-assembled through pnictogen bonding.